

Diversity Gain from a Single-Port Adaptive Antenna Using Switched Parasitic Elements Illustrated with a Wire and Monopole Prototype

Neil L. Scott, Miles O. Leonard-Taylor, Rodney G. Vaughan, *Senior Member, IEEE*

Abstract—A new concept in single-port adaptive antennas using parasitic elements with switched terminating impedances is presented including results from a concept prototype. Each parasitic element can be effectively terminated in three impedance values. The antenna concept provides multiple radiation patterns with a single RF signal port without the need for RF switches or phase shifters in the direct RF signal path. Impedance variations in the active antenna element are minimized by use of only rotationally symmetric configurations. Measured patterns are used to demonstrate the performance improvement expected using switched diversity combining in a simulated uniform scattering scenario. The concept prototype having one active element and four parasitic elements, is shown to have equivalent diversity performance to between three and four uncorrelated branches.

Index Terms—Adaptive, averaged uniform scattering scenario, diversity gain, single-port diversity antenna, switched parasitic antenna elements, wire monopole antenna.

I. INTRODUCTION

IN mobile communications, the radio channel is impaired by the effects of multiple path propagation. The multiple path arises from the transmitted signal illuminating objects in the environment that act as scatterers. The receiving antenna sums the signals from the scatterers with random amplitudes and phases to result in a fading channel.

Switched diversity attempts to improve the effective channel by switching between available channels with uncorrelated fading. These uncorrelated channels are achieved by separating the antenna patterns in space, direction, or polarization. The receiver is conventionally connected by an RF switch to one of the available antennas at a time. This requires a low-loss switch and possibly duplication of some front-end components.

This paper presents an antenna that implements switched diversity combining while requiring only a single RF signal port. It has no switches in the direct received RF signal path and, therefore, requires no duplication of receiver components. The antenna configuration and radiation pattern are controlled by binary inputs which switch the terminations of parasitic elements in the array.

II. SWITCHED PARASITIC CONCEPT

Switched element antennas offering directional patterns have been previously reported, e.g., [1]–[6] and [11].¹ The

Manuscript received June 16, 1997; revised December 14, 1998.

The authors are with the New Zealand Institute for Industrial Research Limited, Lower Hutt, New Zealand.

Publisher Item Identifier S 0018-926X(99)05819-6.

¹ Since submission of this paper, [11] has appeared.

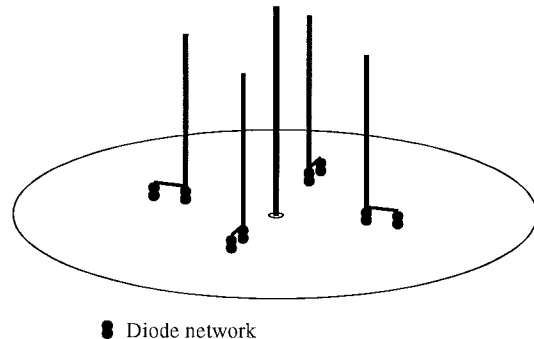


Fig. 1. The structure of the prototype antenna showing the central active element surrounded by parasitic elements with horizontal terminating impedance sections.

concept of the switched parasitic antenna is that active antenna elements do not have to be switched to obtain radiation patterns yielding independent received signals. Milne [2], for example, has previously used switched parasitics for adaptive pattern control for satellite communications.

The concept is here embodied by combining an active antenna element into a structure of parasitic antenna elements that act together to form arrays. One example of this concept would be multiple Yagi–Uda arrays sharing the active element. The termination impedances of the parasitic elements of the array are switchable to change the currents flowing in those elements. The altered currents in turn interact with the active antenna element, modeled by the mutual impedance. The mutual impedance is a function of the physical structure and, therefore, constant. The actions of the changes in currents of each parasitic element and their combined effect on the active element cause the change in radiation pattern.

In this way, multiple radiation patterns with low correlation may be obtained with a single active antenna element. The receiver is always connected to this antenna element so there are no switches in the received RF direct signal path. Control of the parasitic antenna elements is by switching element termination impedances to ground. This prototype uses dc bias to control diodes as the control element. All the diode switches switch to ground simplifying the circuitry.

III. SWITCHED PARASITIC PROTOTYPE

A concept prototype switched parasitic antenna that was constructed is illustrated in Fig. 1, with construction details in Fig. 2. The prototype has not been optimized for any particular physical or performance parameter or application. It is intended solely to illustrate the concepts identified in the abstract,

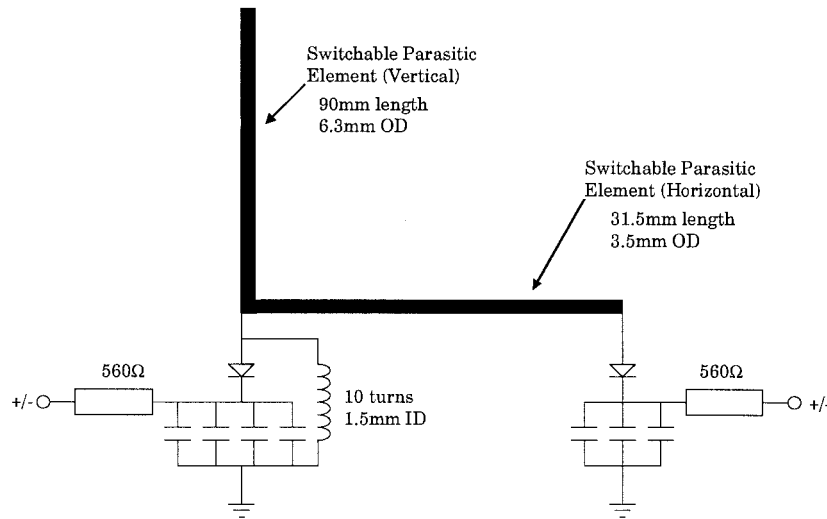


Fig. 2. Element detail of the switched parasitic antenna prototype. Nominal operation is at 851 MHz.

i.e., single port antennas with diversity gain, parasitics with multiple termination impedances, and use of reduced symmetric sets of configurations to prevent impedance changes.

The concept prototype antenna consists of a center active monopole on a groundplane surrounded by four identical symmetrically placed parasitic switchable elements. The ground plane used is 500 mm diameter. The vertical elements are 6.3-mm-diameter copper with lengths 110 and 90 mm. The parasitic vertical elements are at a radius of 92 mm. The horizontal elements are approximately 3.5 mm diameter, 31.5 mm long, and 9.95 mm above the groundplane. All measurements in the paper were performed at 851 MHz. The vertical elements are physically supported by the chip capacitors mounted symmetrically at the base. The switched elements are constructed to be switchable into three distinct states of terminating impedance with two control inputs. A negative bias applied to the input at the knee in the element effectively provides an RF path to the groundplane at this point. The element therefore appears as a “short” monopole. A positive bias at this point and a negative bias at the other input provides an effectively “longer” element with correspondingly different impedance. Positive bias at both inputs effectively makes the element isolated from the groundplane, i.e., open circuited. These terminations make the parasitic element appear as a director, a reflector, or effectively “invisible.”

The vertical polarization is dominant in the prototype. The horizontal sections forming the “longer” terminating impedance of the antenna elements are included in this prototype to aid illustration of the concept. The horizontal radiation pattern of this prototype will therefore change corresponding to the roles of the horizontal elements in each switching configuration. This horizontal polarization radiation is not discussed here as these effects are not central to the discussion and could be eliminated in other implementations such as by mounting the termination impedance below the groundplane.

IV. MEASURED ANTENNA PATTERNS

Directional radiation patterns can be constructed with the prototype by switching the parasitic elements to various com-

binations of terminations. With four switchable elements capable of three impedance states each, there are 3^4 possible configurations for the parasitic elements. These various configurations will result in changes to the impedance seen by the active element. This situation is avoided by restricting the allowed configurations to rotational and reflected symmetry variants on principal configurations [7].

Associating the antenna directions with north, west, south, and east, a north pointing pattern can be selected by selecting the “N” element to be director and the “S” element to act as a reflector. If the antenna elements corresponding to “W” and “E” are switched to their isolated state they will have minimal effect on the overall radiation pattern. The four-way symmetry of the prototype suggests that patterns created in this way can be fabricated in each of the cardinal directions and nearly identical patterns and impedances can be expected. Patterns in the four intercardinal directions can be constructed by selecting two adjacent elements for each of the selected states. For example, selecting the “S” and “E” elements to be directors and the “N” and “W” to be reflectors creates a directional pattern oriented toward southeast (SE).

Some of the possible radiation patterns available from the prototype antenna were measured in an anechoic chamber. Fig. 3 shows the measured radiation patterns for each of the major directions, N, S, E, W, and one minor direction SE generated as outlined above. The small amount of asymmetry seen in the measured patterns is attributed to physical asymmetry’s in the construction of the prototype. The measured half-power beam widths are 124° , 99° , 119° , 104° , and 100° , respectively.

Under certain conditions, the normalized crosscorrelation functions of the receiving antenna patterns are related to the cross correlation of the received signals from the antennas [7], [8]

$$\begin{aligned} \rho_{12} &= \langle V_{O1} V_{O2}^* \rangle \\ &= \int_0^{2\pi} \int_0^\pi S(\theta, \phi) g_1(\theta, \phi) g_2^*(\theta, \phi) \sin \theta d\theta d\phi \quad (1) \end{aligned}$$

where the g_1 and g_2 are the normalized receiving patterns of the antennas and S is the distribution of incident waves.

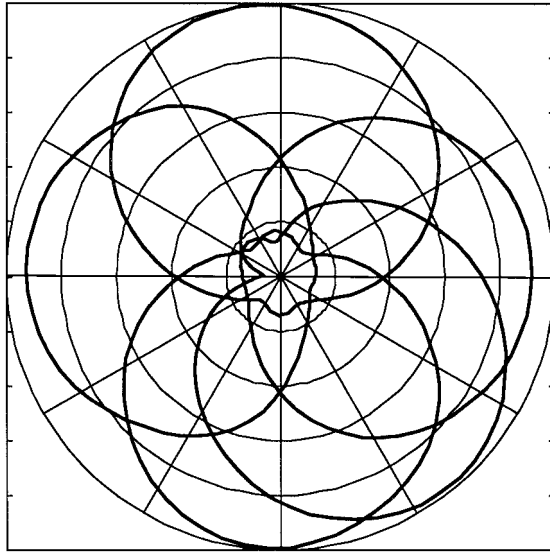


Fig. 3. Measured azimuthal patterns of the switched parasitic antenna patterns. The patterns have been normalized to the maximum value of the five patterns displayed (here the "north" pattern) and are displayed on a linear scale—the center being zero. Of the intercardinal direction patterns only the "southeast" pattern is shown.

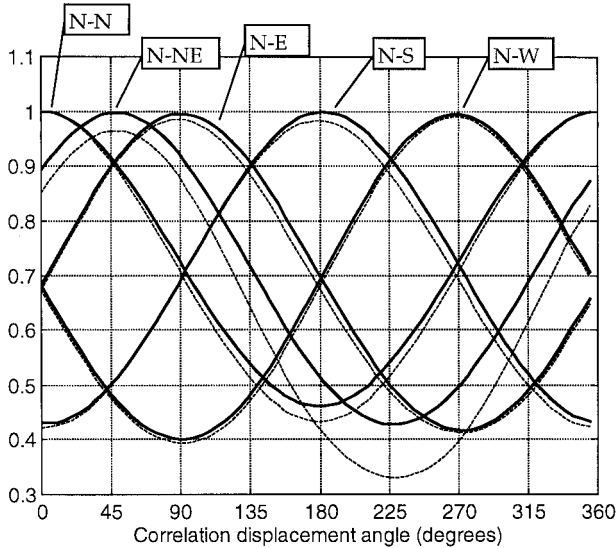


Fig. 4. Cross correlation coefficients of magnitude patterns $\rho_{|n||x|}$ (solid) and magnitude of cross correlation for complex patterns $|\rho_{nx}|$ (dashed) between the north pattern and the other directions.

The distribution discussed in this paper is the uniform dense scatterer environment modeled by the Clarke simulator for which $S(\phi)$ is constant, i.e., without directional dependence. The simulations and measured patterns in this paper are restricted to the horizontal plane.

Fig. 4 shows the cross correlation of one pattern N with the others. The solid curves are the real correlations calculated from the antenna magnitude patterns

$$\rho_{12}(\phi_0) = \int_0^{2\pi} \left| g_1\left(\frac{\pi}{2}, \phi\right) \right| \left| g_2^*\left(\frac{\pi}{2}, \phi + \phi_0\right) \right| d\phi. \quad (2)$$

The dashed curves correspond to the magnitude of the correlation using the complex patterns. The correlations using the

complex patterns are always lower than those with magnitude alone but are very close. This similarity indicates that the correlation mechanism involved between these patterns is predominantly magnitude based.

The high-peak cross correlation values at 45° , 90° , 120° , and 270° reflect the pattern similarity that is to be expected from symmetry considerations. The minimum value of the correlation with the 45° pattern (here NE) is lower than those of the major direction patterns. This reflects the different antenna configuration required to generate the intercardinal patterns. The configuration difference results in a very similar pattern magnitude but somewhat different pattern phase.

Following [9], the correlation coefficient between the Rayleigh-distributed envelopes of the received signals approximately equals the square of the correlation coefficient for the signals themselves, i.e., $\rho_e \approx |\rho_{12}|^2$. For diversity combining, a practical requirement for decorrelated envelopes is taken as $\rho_e \approx 0.7$ or $|\rho_{12}| \approx 0.85$. The correlation coefficients of the cardinal direction patterns falls to $|\rho_{12}| \approx 0.85$ at a correlation angle displacement of about 60° . At 90° correlation angle displacements, $\rho_e \approx 0.5$ showing that the cardinal direction patterns (N, E, S, and W) are expected to provide good diversity action. The adjacent 45° patterns (e.g., N and NE) have $\rho_e \approx 0.8$ and a correspondingly reduced diversity gain.

V. SIMULATIONS

The radiation patterns measured from the prototype antenna were used in a multiple path simulator to investigate the performance of the antenna in a dense multiple path scenario. The simulator was designed as a two-stage process to provide maximum flexibility. In the first stage, a modified Clarke scenario is used to produce a Rayleigh multiple-path fading environment. The simulator reads files representing the patterns measured for the prototype antenna before simulating movement of antennas with those patterns while traveling east through the fading environment. The simulations used 20 signal sources and a total mobile travel of approximately 310 wavelengths. The complex amplitudes of the signals that would be received by each of the available antenna radiation patterns are logged for later processing in the second stage. This approach allowed the signals from all possible antenna configurations to be examined and combined repeatedly. All the signals are not available simultaneously from the actual prototype antenna as only one radiation pattern can be selected at a time.

The second stage of the simulator combines the signals to produce the signal that would be seen from an adaptive antenna/receiver pair. The simulated adaptive receiver measures the received signal amplitude as a performance index. When the amplitude falls below a threshold the receiver switches to another antenna configuration.

A. Received Signal Crosscorrelation Coefficients

Table I lists the cross correlation coefficient values for squared signal envelopes $\rho_e \approx \rho_{r_1 r_2}^2$ for all combinations of the possible received patterns. For example the cross

TABLE I

POWER CORRELATION COEFFICIENT ESTIMATES FOR THE POSSIBLE RECEIVING PATTERNS. THE SAMPLES USED TO CALCULATE THESE VALUES ARE FROM A SIMULATION OVER A DISTANCE OF APPROXIMATELY 310 WAVELENGTHS. THE PRESENCE OF SOME NEGATIVE SAMPLE VALUES INDICATE THE EFFECT OF THE FINITE LENGTH SAMPLE WINDOW

Direction	Angle displacement of beams			
	+45°	+90°	+135°	+180°
N	0.7	0.4	0.0	-0.1
NE	0.7	0.2	0.0	-0.0
E	0.6	0.4	0.2	0.2
SE	0.9	0.4	0.2	-0.1
S	0.8	0.4	-0.1	
SW	0.6	0.0	-0.1	
W	0.6	0.4	0.2	
NW	0.8	0.4	0.2	

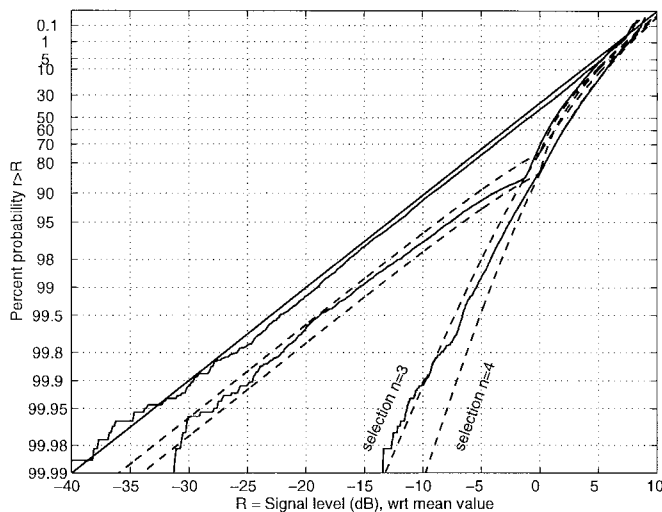


Fig. 5. Rayleigh plot of the signal received by one antenna pattern and the combined signals. The dashed curves show theoretical performance for switched and selection combining for three and four independent branches.

correlation of the N and NE patterns appears in the table in the N row and +45° column. The correlation values corresponding to pattern separations of 45° are high as predicted by the high correlation of adjacent patterns. The values corresponding to 90° separation agree well with the 0.5 predicted from the patterns.

B. Received Signal Amplitude Improvement

Fig. 5 shows a plot of the cumulative probability distributions of the antenna signal envelopes on Rayleigh axes. The plot shows the signal from one of the individual antenna configuration radiation patterns and combined signals referenced to the overall mean level.

A curve representing the performance of a selection combiner operating on the same signals is included for comparison. Previously derived reference curves [10] for three and four branch switched diversity combining and three branch selection diversity are included. All these reference curves are for uncorrelated branch signals. The signal that would have been received by the individual antenna configuration can be seen to follow closely the Rayleigh reference line as expected. The control algorithm switched the antenna configuration whenever the sample of the received signal envelope fell below the mean

level of all the signals over the simulation. The mean level estimate was available accurately because of the two stage nature of the simulation. In real implementations the mean would have to be estimated from prior samples only, if required by the threshold algorithm. Switching between antenna configurations is modeled as instantaneous. After switching, the receiver produces a sample of the signal received by the new antenna configuration on the next sample.

Comparing the selection diversity combined reference curves and that from the simulation suggests that the eight partially correlated signals from the antenna are approximately equivalent to four uncorrelated branches. The switched combining curves for four uncorrelated branches show similar agreement. A significant diversity gain can be achieved with a simple, easily controlled, antenna without highly directive radiation patterns.

VI. CONCLUSION

The switched parasitic antenna prototype demonstrates a concept for implementation of adaptive diversity antennas. The antenna concept has the potential to provide multiple uncorrelated radiation patterns (or multiple correlated patterns) with a single RF feed point and no RF switches in the signal path.

Switched parasitic antenna elements that have three states of termination impedance have been demonstrated in a hardware prototype. The multiple state elements allow control of antenna configuration with binary inputs. The number and diversity of patterns available with three state elements is increased over two state elements without significantly increasing the complexity of the antenna implementation or the required volume. The increased number of patterns allows more freedom to choose patterns related by symmetry to control the impedance seen by the active receiving element.

A concept prototype has been constructed and radiation patterns measured. No attempt has been made to minimize the size of this concept prototype antenna nor to optimize the design for any physical or performance parameter or application. The measured patterns applied in multiple-path fading simulations have shown that prototype antenna performance is approximately equivalent to that expected of a switched combining scheme operating with between three and four completely uncorrelated antenna patterns.

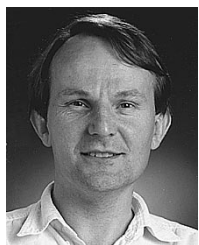
ACKNOWLEDGMENT

The authors would like to thank C. Jenness of the Communications Group of The New Zealand Institute for Industrial Development for his able assistance during the course of this work.

REFERENCES

- [1] M. Gueguen, "Electronically step-by-step rotated directive radiation beam antenna," U.S. Patent 3 846 799, 1974.
- [2] R. M. T. Milne, "A small adaptive array antenna for mobile communications," in *IEEE Antennas Propagat. Symp. Dig.*, June 1985, pp. 797-800.

- [3] T. A. Dumas and L. V. Griffee, "Electronically rotated antenna apparatus," U.S. Patent 4 631 546, Dec. 1986.
- [4] D. V. Thiel, S. G. O'Keefe, and J. W. Lu, "Electronic beam switching in wire and patch antenna systems using switched parasitic elements," in *IEEE Antennas Propagat. Soc. URSI Radio Sci. Meet.*, Baltimore, MD, July 1996, pp. 534–537.
- [5] S. L. Preston, D. V. Thiel, J. W. Lu, S. G. O'Keefe, and T. S. Bird, "Electronic beam steering using switched parasitic patch elements," *Electron. Lett.*, vol. 33, no. 1, pp. 7–8, Jan. 1997.
- [6] A. Sibille, C. Roblin, and G. Poncelet, "Circular switched monopole arrays for beam steering wireless communications," *Electron. Lett.*, vol. 33, no. 7, pp. 551–552, Mar. 1997.
- [7] R. G. Vaughan, "Switched parasitic elements for antenna diversity," *IEEE Trans. Antennas Propagat.*, vol. 47, pp. 399–405, Feb. 1999.
- [8] R. G. Vaughan and A. J. Bach, "Antenna diversity in mobile communications," *IEEE Trans. Veh. Technol.*, vol. VT-36, pp. 149–172, Nov. 1987.
- [9] J. R. Pierce and S. Stein, "Multiple diversity with nonindependent fading," *Proc. IRE*, vol. 48, pp. 89–104, 1960.
- [10] W. C. Jakes, *Microwave Mobile Communications*. New York: IEEE Press, 1974.
- [11] S. L. Preston and D. V. Thiel, "Direction finding using switched parasitic antenna array," in *IEEE Antennas Propagat. Soc. Int. Symp.*, Montreal, Canada, July 1997, pp. 1024–1027.



Neil L. Scott received the B.E. and M.E. degrees in electrical engineering from the University of Canterbury, New Zealand, in 1979 and 1981, respectively.

After graduating, he worked in the New Zealand Electricity Department, for four years in the area of remote control, metering, data acquisition for hydropower stations, systems engineering, and applications of microprocessors. Transferring to the then Department of Scientific and Industrial Research (DSIR), he worked on software for a personal computer based clinical tool. With the formation of the Communications Team, he worked on sampling theory, multiple-path radio propagation mechanisms, computer simulation, and indoor and outdoor radio measurements. In 1992 with the restructure of the DSIR into Crown Research Institutes, he transferred to the New Zealand Institute for Industrial Research and Development (IRL), Wellington. His research topics have included simulation of communications processes, signal processing, DSP implementation issues, and novel antennas. His involvement in recent developments for the industry has included applications of DSP for audio signal processing functions, global positioning system (GPS), computer simulation of communications processes, and development of real-time systems.

Miles O. Leonard-Taylor received the the New Zealand Certificate in Engineering (NZCE) from Wellington Polytechnic, in 1989.

He worked for the Department of Scientific and Industrial Research and continued following its restructure into the New Zealand Institute for Industrial Research, in 1992. His recent industrial development work has included implementation of digital signal processing functions in hardware, software engineering for real-time embedded systems, and development of manufacturing prototypes for personal communication systems antennas. Current research interests include digital simulation of multiple path propagation, antenna systems and communications systems, signal processing for super-resolution of channel sounding signals, and pole-zero modeling of time signals.

Rodney G. Vaughan (M'84–SM'89), for a photograph and biography, see p. 990 of the July 1998 issue of this TRANSACTIONS.